NUMERICAL ANALYSIS OF THE FLOW CONDITIONS IN THE AIR DISTRIBUTION ELEMENT

MARIA CARNOGURSKA[1], MIROSLAV PRIHODA[2], DANIELA POPCAKOVA[1]

[1]Department of Power Engineering, Faculty of Mechanical Engineering, Technical University of Kosice, Kosice, Slovak Republic

[2]Department of Thermal Engineering, Faculty of Materials Science and Technology, VSB Technical University of Ostrava, Ostrava, Czech Republic

DOI: 10.17973/MMSJ.2020_10_2020015

maria.carnogurska@tuke.sk

The article presents the results of a numerical analysis of the flow conditions in the air distribution element in a combined refrigerator and freezer. A numerical analysis was carried out using the boundary conditions identified through an experiment. The article includes an analysis of the impact of the mesh type and the used turbulence models on the profile of the air flow velocity in the outlet openings of the used distribution element. The required ratio of the volumetric flow rates of the air absorbed by the fan, for the smaller to the larger outlet openings, should be 1:2.2. This air distribution ratio was monitored using three turbulence models: the SST model, the *k-ε* model and the RNG model, and two types of elements: tetrahedron and hexahedron, or combinations thereof. The obtained results were used as the basis for a modification of the geometry of the distribution element itself, and a concurrent modification of the size of the gap between the impeller and the internal space of the device.

KEYWORDS

air distribution element, velocity conditions, numerical analysis, computational fluid dynamics, turbulence models

1 INTRODUCTION

At present, the complicated tasks regarding heat transfer [Čarnogurská 2011], [Junga 2019], [Rimár 2020] and flow [Bardina 1977], [Čarnogurská 2009], [Kozubková 2019] are dealt with by applying the numerical mathematical methods integrated in various simulation software programs. However, the applications of computational fluid dynamics are not subject to any limitations [Caughey 2002]. The validation, testing and development, especially in the field of turbulent phenomena, have received a great attention for many years; for example, in the paper [Bardina 1997]. Researchers and manufacturers of various technological devices make use of the features provided by numerical simulations, based on the Finite Element Method (FEM) and the Finite Volume Method (FVM). In addition to the above-mentioned applications of numerical mathematical methods, they are also used in the field of linear and non-linear statics or dynamics [Bocko 2017], as well as electrotechnology [Kyslan 2017].

2 MATERIAL AND METHODS

In order to obtain information on the flow conditions and the velocity distribution in the outlet openings of the air distribution element in a combined refrigerator and freezer (Fig. 1), extensive experimental research and a simulation of the flow conditions inside the device, including the fan, were carried out. The obtained results were used as the basis for the optimisation of the device shape, with the aim of achieving the most even output velocity of the air flowing from both outlet openings.

The distribution device was divided into two computation zones:

- Computation Zone 1 represented the air with a temperature of 25 °C and the fan impeller (Number **1** in Fig. 1),
- Computation Zone 2 represented the air of the same temperature and the stationary part of the distribution device (Number **2** in Fig. 1).

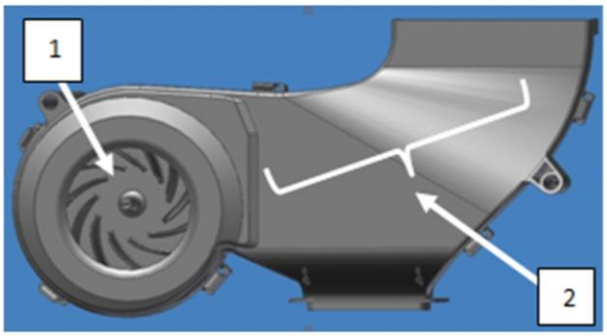

Figure 1. Analysed air distribution element

The required condition for the resulting flow in the distribution element is achieving the state when the volumetric air flow rates from the outlet openings (designated B1 and B2 in Fig. 2) are in the ratio of 1:2.2 [Popčáková 2012]. This should not be accompanied by any changes to the inner shape of the object.
In order to stabilise the air flow before it enters the fan, the impeller geometry was supplemented with a 30 mm long cylindrical socket (designated A in Fig. 2), and the outlets of both openings of the stationary part of the device were supplemented with 60 mm long blocks (designated B1 and B2 in Fig. 2).

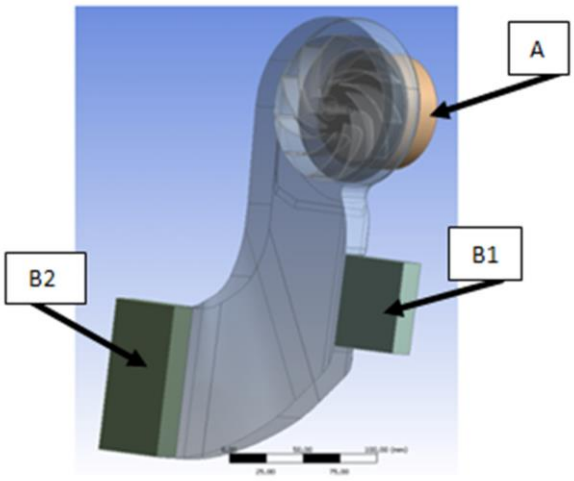

Figure 2. Supplemented device parts

The simulation of the flow conditions was carried out using ANSYS CFX software. The boundary conditions were identified experimentally, by measuring the volumetric flow rate of the

air entering the fan, the air temperature and the air humidity. The volumetric flow rate at the fan inlet was identified by applying three different methods:

- an ultrasonic flow meter (Fig. 3);
- a rotating-vane-anemometer-probe (RP); and
- a CTA (Constant Temperature Anemometer) sensor.

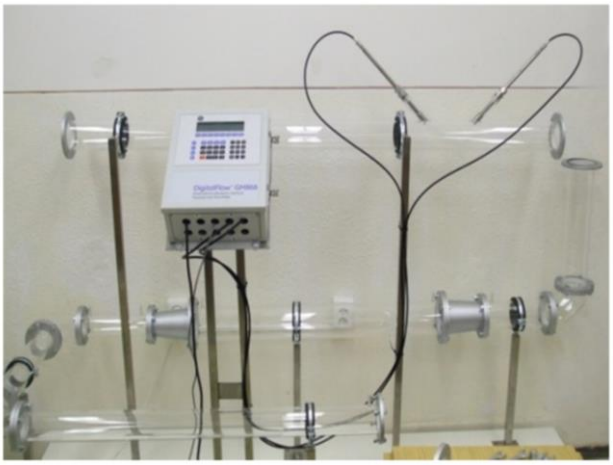

Figure 3. Measurement route with the GM868 ultrasonic flow meter

The identification of the volumetric flow rate using the ultrasonic flow meter consisted of measuring the change in the time for the signal transmission in the flowing fluid. The mean fluid flow velocity was calculated with the following formula:

$$v_{mean} = \frac{c^2}{2 \cdot L \cdot \cos\alpha} \cdot (t_{2,1} - t_{1,2}) \quad (1)$$

where L is the distance between two electroacoustic converters (EC1, EC2) located on the piping (m); α is the angle between the direction of the transmitted signal and the fluid flow direction (°); $t_{2,1}$ is the time of the signal transmission between the converters EC2 and EC1; $t_{1,2}$ is the time of the signal transmission between the converters EC1 and EC2 (s); and c is the velocity of the ultrasonic signal transmission, which is calculated as follows:

$$c = \frac{2 \cdot L}{t_{1,2} + t_{2,1}} \quad (2)$$

In practice, the mean fluid flow velocity is identified using only the signal transmission times $t_{1,2}$ and $t_{2,1}$, by applying the following formula:

$$v_{mean} = k \frac{t_{2,1} - t_{1,2}}{(t_{1,2} + t_{2,1})^2} \quad (3)$$

Where k is the constant of proportionality of the gauge ($k = 2 \cdot L / \cos\alpha$).

The average velocity measured by the ultrasonic measuring device was 2.65 m·s^{-1}. The measured velocity was used to identify the volumetric flow rate Q_V, which was then used to calculate the mass flow rate Q_m = 0.0139 kg·s^{-1}.

The results of the velocity measurements carried out using the vane probe at nine locations before the air entered the fan (Fig. 4) are listed in Table1. The diameter of the inlet opening in the pipe attached to the fan was d = 77 mm. The velocities were measured in the gravity centres of individual partial surfaces. The measurements were repeated four times.

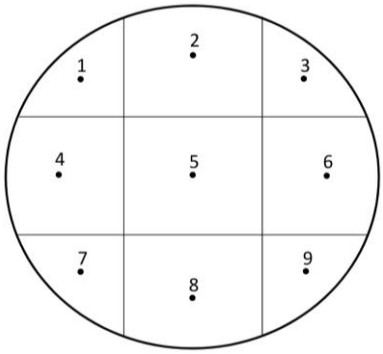

Figure 4. Measurement locations before the fan inlet

Measurement location	Measurement			
	1	2	3	4
1	2.43	2.74	2.44	2.63
2	2.59	2.47	2.47	2.55
3	2.89	2.73	2.56	2.83
4	2.63	2.64	2.77	2.62
5	2.72	2.71	2.79	2.51
6	2.96	2.68	2.68	2.45
7	2.87	2.56	2.65	2.54
8	2.99	2.73	2.45	2.58
9	2.81	2.88	2.79	2.71

Table 1. Air velocity at the fan inlet

The mean value of the air velocity at the fan inlet, as measured using the vane probe, was 2.67 m·s^{-1}.

The average velocity at the fan inlet, as measured using the CTA sensor at the individual points shown in Fig. 4, represented the value of 2.67 m·s^{-1}.

The velocity in the outlet openings of the distribution element (B1, B2 in Fig. 2) was measured at 24 measurement locations along the height of the small opening, and at 39 measurement locations along the height of the large opening. The dimensions of the small opening in the distribution element were 70 x 18 mm, and the size of the large opening was 115 x 18 mm. The measurements were repeated five times and were carried out using the following instruments:

- CTA sensor;
- rotating-vane-anemometer-probe; and
- anemometer (A).

The average velocity values measured using the above-listed means are summarised in Table 2.

Measuring device	Outlet opening B1	Outlet opening B2
	v (m·s^{-1})	v (m·s^{-1})
CTA sensor	3.19	4.28
RP	2.54	3.28

A	2.92	4.22

Table 2. Comparison of the velocity values measured using the CTA, RP and A

The comparison of the measurement results, primarily at the outlet openings, indicates significant differences between the measured velocity values.

Therefore, the mean velocity of the air flowing in both openings was also identified by applying the numerical method. The simulation was carried out in the ANSYS CFX environment [Kozubková 2016].

3 NUMERICAL ANALYSIS

The numerical analysis of the flow conditions was carried out using three types of models integrated with the ANSYS CFX software: *the SST model*, *two-equation model k-ε and the RNG model.* Each model has specific characteristics and is suitable for a certain type of the solved task. Two mesh types were used with each model: tetrahedral mesh and hexahedral mesh. The focus of the testing was the impact of the mesh type on the distribution of the flow fields, separately for both Computation Zones, as shown in Fig. 1.

The boundary condition at the fan inlet was the mass flow rate, which was identified on the basis of the velocity measurement using the ultrasonic flow meter.

In the Alternative 1, tetrahedral mesh was used for both Computation Zones. The impact of the mesh type employed was analysed for all three turbulence models.

In the Alternative 2, hexahedral mesh was used for Computation Zone 1 (Number 1 in Fig. 1) and the tetrahedral mesh was used for the Computation Zone 2 (Number 2 in Fig. 1). Again, all three models were used in this solution.

With regard to the Alternative 1, the results of the numerical simulation are shown in Figs. 5 through 7.

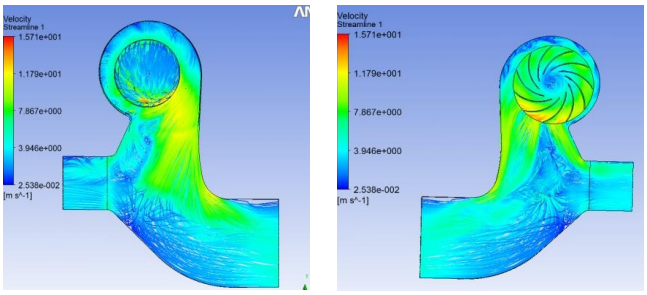

a) air inlet side of the fan and the device openings

b) air outlet side of the fan and the device openings

Figure 5. Streamline shapes in the Alternative 1 - SST model

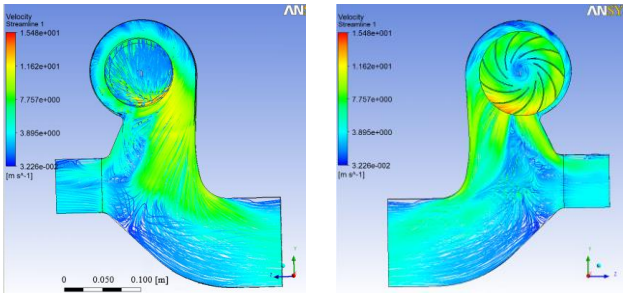

a) air inlet side of the fan and the device openings

b) air outlet side of the fan and the device openings

Figure 6. Streamline shapes in the Alternative 1 - RNG model

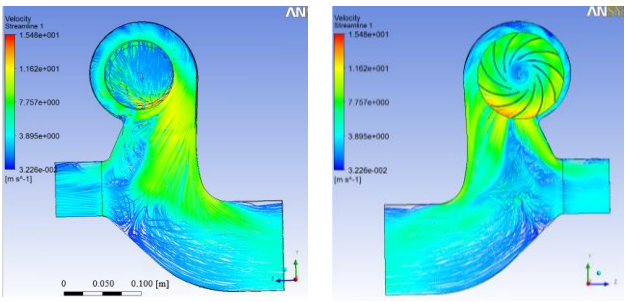

a) air inlet side of the fan and the device openings

b) air outlet side of the fan and the device openings

Figure 7. Streamline shapes in the Alternative 1 - *k-ε* model

A comparison of the simulation results shown in Figs. 5 through 7 indicates that the velocity distributions in the device are comparable in all three models. The local air flow turbulence was different only in the central part of the device. The highest velocity was observed in the outlet part of the fan when the SST turbulence model was used (15.71 $m \cdot s^{-1}$). When the *k-ε* model was used, the value was 15.48 $m \cdot s^{-1}$, and with the RNG model it was 15.54 $m \cdot s^{-1}$.

The summary of the mean flow velocities at the outlets from both monitored openings, with the use of the tetrahedral mesh and all three turbulence models, is presented in Table 3.

Model type	Opening B1	Opening B2
	v ($m \cdot s^{-1}$)	v ($m \cdot s^{-1}$)
SST model	3.14	4.24
k-ε model	3.18	4.32
RNG model	3.19	4.33

Table 3. Mean velocities identified using the models – Alternative 1

The table indicates that the mean velocity values did not depend very much on the used type of the turbulence model.

When simulating the flow conditions in rotary devices, such as fans, pumps etc., it is recommended that mesh created from hexahedral elements is used, as it facilitates obtaining more accurate results [Bardina 1977]. However, for an object, a mesh created from tetrahedral elements may be used. This type of mesh is also suitable for more complex geometrical shapes.

In Alternative 2, the maximum velocity observed at the outlet from the fan was 14.73 $m \cdot s^{-1}$ with the use of the SST model, as well as with the RNG model. In the case of the *k-ε* model, the observed maximum value was in fact identical, at 14.7 $m \cdot s^{-1}$.

A summary of the mean flow velocities at the outlets from both monitored openings in Alternative 2 is shown in Table 4.

Model type	Opening B1	Opening B2
	v ($m \cdot s^{-1}$)	v ($m \cdot s^{-1}$)
SST model	2.92	4.15
k-ε model	2.97	4.15
RNG model	2.93	4.16

Table 4. Mean velocities identified using the models – Alternative 2

The mean values observed while applying all three turbulence models were practically identical.

4 MODIFICATION OF THE INTERNAL SPACE OF THE DISTRIBUTION ELEMENT

The simulation results for Alternative 2 exhibited better accordance with the values obtained experimentally. Therefore, subsequent solutions were made using the elements selected in Alternative 2, i.e. hexahedron in the inlet zone and tetrahedron in the outlet zone.

On the basis of the mean values obtained from the simulation, the ratios of air flow rates in the outlet openings were assessed. The value of the arithmetic average of the velocities for both openings, as shown in Table 4, was substituted for the mean velocity. The flow area of the small opening in the distribution element was $S_1 = 1.26 \cdot 10^{-3}$ m^2; while for the large opening it was $S_2 = 2.07 \cdot 10^{-3}$ m^2. The mean flow velocity in the small opening was 2.94 m·s^{-1}; and in the large opening it was 4.15 m·s^{-1}. The volumetric flow rate in the small opening represented a value of $3.70 \cdot 10^{-3}$ m^3·s^{-1}; whereas in the large opening it was $8.60 \cdot 10^{-3}$ m^3·s^{-1}. The ratio of the flow rates was 1:2.32.

The aforementioned facts indicate that, in order to achieve the required ratio of 1:2.2 for the flow rates in the small and large openings, the inner space of the distribution element had to be subjected to a modification. The proposed solution was to install straight, 1 mm thick guiding components before the outlet openings – four components before the large opening, and three components before the small opening. A simulation was carried out using the *k-ε* model, with the combined tetrahedral and hexahedral elements. The observed pattern of the flow from the outlet openings did not exhibit any marked increase in the evenness (Fig. 8).

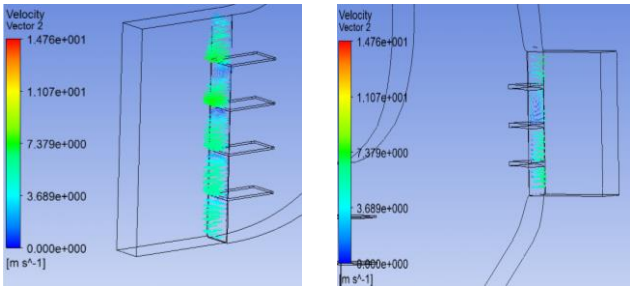

a) velocity distribution in the large opening

b) velocity distribution in the small opening

Figure 8. Velocity distributions in the outlet openings of the device – straight guiding components

This was caused by inappropriate aerodynamic conditions after installing the straight components in the device. Therefore, several different alternatives to the air guiding plates were tested. Seemingly the most efficient solution was the installation of 4 shaped 1 mm thick plates, immediately before both outlet openings. The distribution of the velocities along the height of both openings, with the same turbulence model *k-ε* and the same mesh type, may be seen in (Fig. 9). In this case, the flows from both openings were more even; but despite these efforts, the required ratio of the flow rates was not achieved.

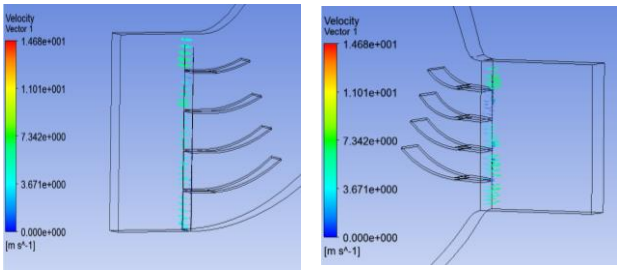

a) velocity distribution in the large opening

b) velocity distribution in the small opening

Figure 9. Velocity distributions in the outlet openings of the device – shaped guiding components

Another modification to the distribution element was a change in the size of the gap between the fan and the internal space of the distribution element. Such a modification was expected to result in a more appropriate air flow distribution already in the impeller, and this would also result in achieving the required distribution into the outlet openings. The size of the gap was changed through two alternatives – with gap sizes of 0.5 mm and 1 mm. None of the proposed modifications brought the required result. Therefore, several structural changes were made in the stationary part of the object. Fig. 10a shows a substantial change in the method how the flow was guided by removing a "*dead*" part of the guiding plate. The final shape of the distribution element is shown in Fig. 10b. Changes were also observed in the heights of the small and large openings. Several additional simulations revealed that the required ratio 1:2.2 of the flow rates may be achieved by reducing the height of the small opening from 70 mm to 45 mm and of the large opening from 115 mm to 71 mm, while simultaneously maintaining the width of both openings at 18 mm and a gap height of 0.5 mm. The volumetric flow rate in the small opening after such changes represented approximately 0.00846 m^3·s^{-1}.

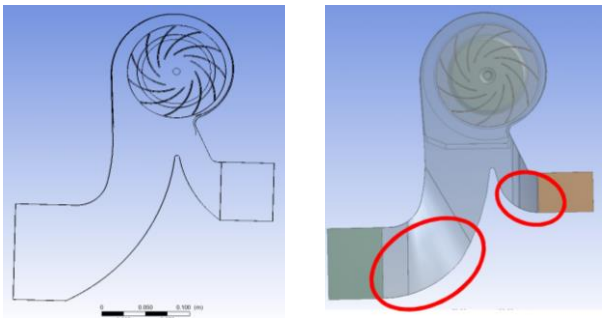

a) basic modification of the device shape

b) additional modification of the device shape

Figure 10. Modification of the device with a concurrent change of the gap height of 0.5 mm

5 CONCLUSIONS

The numerical analyses of the air distribution element in the combined refrigerator and freezer facilitated a detailed analysis of this device.

The analysis was based on an assessment of the suitability of the SST, *k-ε* and RNG turbulence models and the mesh types – tetrahedral or hexahedral. All the simulation results were compared with the velocity values obtained experimentally using a CTA sensor, a vane probe and an anemometer.

The obtained results were used to perform modifications of the distribution element, so that the flow rates in both outlet

openings reached the required ratio of 1:2.2, which was also the manufacturer's requirement. The presented design facilitated increasing the velocity in the outlet openings, and this had a very positive effect in terms of the cooling performance. Also, the flowing air was homogenised along the cross-section and, as the most important result, the required ratio of the flow rates in both outlet openings was achieved. The results of this solution have been submitted to the relevant representatives of the manufacturing company.

ACKNOWLEDGMENTS

The paper has been produced as a part of the VEGA No. 1/0626/20 and SP 2020/34-FMT VŠB TUO projects.

REFERENCES

[Bardina 1977] Bardina, J. E., Huang, P. G. Coakley, T. J. Turbulence modeling validation, testing, and development, NASA Technical Memorandum 110446, 1997. pp. 88.

[Bocko 2017] Bocko, J., Lengvarsky, P. Buckling of single-walled carbon nanotubes with and without defects. J. Mech. Sci. Technol., vol. 31, no. 4, 2017, pp. 1825-1833.

[Caughey 2002] Caughey, D. A., Hafez, M, M. Frontiers of computational fluid dynamics, 2002. World Scientific Publishing, New Jersey-London-Singapore-Hong Kong, 2002. ISBN 981-02-4849-0.

[Carnogurska 2009] Carnogurska, M., Prihoda, M., Popcaková, D. Modelling the flow conditions in the tunnel and its reduced model. J. Mech. Sci. Technol., vol. 24, no. 12, 2010. pp. 2479-2486.

[Carnogurska 2011] Carnogurska, M., Prihoda, M., Molinek, J. Determination of deposit thickness in natural gas cooler based on the measurements of gas cooling degree. J. Mech. Sci. Technol., vol. 25, no. 11, 2011 pp. 2935-2941.

[Junga 2019] Junga, P., Travnicek, P., Ruzbarsky, J. Impact of thermal bridges on thermal properties of the old poultry houses structures. MM Science Journal, 2019, December, pp. 3445-3452.

[Kozubkova 2019] Kozubkova, M., Jablonska, J., Bojko, M., Dvorak, L., Carnogurska, M. Multiphase fluid models to deal with fluid flow Dynamics, MM Science Journal, 2019, December, pp. 2892-2896.

[Kozubkova 2016] Kozubkova, M. et al. Computer modeling I (in Czech). Ostrava, VŠB-TU, 2016. Available from <http://www.338.vsb.cz/studium/studijni-opory/>

[Kyslan 2017] Kyslan, K., Rodic, M., Suchy, L., Ferkova, Z., Durovsky, F. Industrial controller-based dynamometer with dynamic emulation of mechanical loads. Electrical Engineering. vol. 99, no. 4 (2017), pp. 1245-1254.

[Popcakova 2012] Popcakova, D. Optimization of flow parameters in selected cooling system (in Slovak). Dissertation thesis, Kosice, TUKE, 2012.

[Rimar 2020] Rimár, M., Kulikov, A., Fedak, M., Khovanskyi, S., Pavlenko, I. Application of the CFD software for modeling thermal comfort in sport hall. MM Science Journal, 2020, March, pp. 3723-3727.

CONTACTS:

prof. Ing. Maria Carnogurska, CSc.
Technical University of Kosice, Faculty of Mechanical Engineering, Department of Power Engineering,
Vysokoskolska 4, SK – 04022 Kosice
+421 55 602 4357, maria.carnogurska@tuke.sk